ACS Photonics

Letter

pubs.acs.org/journal/apchd5

Effective Wavelength Scaling of and Damping in Plasmonic Helical Antennae

José M. Caridad,[†] David McCloskey,[†] Francesco Rossella,[‡,§] Vittorio Bellani,[‡] John F. Donegan,[†] and Vojislav Krstić*[,†,∥]

[∥]Department of Physics, Chair for Applied Physics, Friedrich-Alexander-University Erlangen-Nürnberg (FAU), Staudtstr. 7, 91058 Erlangen, Germany

[†]School of Physics, CRANN, AMBER Research Centre, Trinity College Dublin, College Green, Dublin 2, Ireland

[‡]Dipartimento di Fisica "A. Volta", Università degli Studi di Pavia, via Bassi 6, 27100 Pavia, Italy

[§]NEST, Instituto Nanoscienze-CNR and Scuola Normale Superiore, Piazza S. Silvestro 12, 56127 Pisa, Italy

Supporting Information

ABSTRACT: We report on the optical performance of metallic nanohelices as the extension of the helical antenna concept into the optical wavelength range. These helical nanoparticles exhibit a structure and material dependent optical response due to the existence of a longitudinal localized-plasmon resonance which scales linearly with the total length of the helix; thus, comprising the number of turns and the single-turn length of the nanohelix. This is in contrast with macroscopic metallic helices, where the scaling of their operational mode is only determined by the length of a single turn. We show how the plasmon damping is radiated or absorbed depending on the interband activity of the metal forming the nanohelix. This study demonstrates the ability of helical structures to control and manipulate optical fields at the nanometer scale according to their specific shape and material composition.

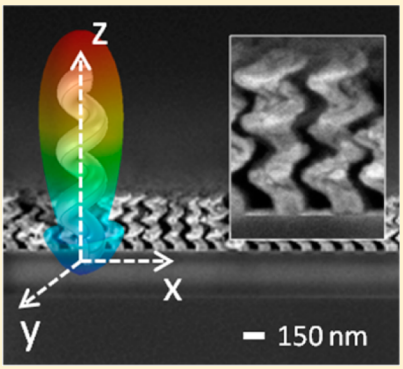

KEYWORDS: *metallic nanohelices, plasmonic antenna, optical antenna, wavelength scaling, glancing angle deposition, plasmonic damping*

Metallic helical structures with feature-sizes in the micrometer and larger ranges constitute an interesting antenna shape. They function as a directional antenna radiating waves along the antenna's axis when the length of one turn of the helix is comparable to the radiation wavelength (so-called axial mode).[1] They are widely used in many applications including radio frequency and microwave-transceivers[1] and as circular polarizers in the mid-infrared.[2] In addition, they are part of rectifier/antenna-circuits for energy-harvesting applications in the radio frequency and microwave ranges.[3] Plasmonic antennae with feature sizes on the nm-scale are the optical counterpart of microwave and radiowave antennas, enabling the control and manipulation of optical fields at the nanometer scale.[4,5] Nevertheless, they have important differences with respect to their macroscopic analogues related to their size and resonant properties of metal nanoparticles at optical frequencies.[4,5] Several shapes of antennae have been studied at the nanoscale, mainly focusing on simple geometries or on particles with similar shape to a macroscopic equivalent. Examples are spheres,[6] ellipsoids,[6] disks,[7,8] nanorods,[9] bowtie,[10] monopole,[11] dipole,[12] and Yagi-Uda[13] types of nanostructures. However, helical antennae have not yet been intensively exploited in the optical spectrum due to the lack of structurally well-defined metallic helical objects of nanometer size.[4,5] We recently reported on a controlled technique that enables the achievement of freestanding, regular shaped, and multiple-turn metallic nanohelices at room temperature conditions[14] using oblique physical evaporation techniques[15] with pitches below 100 nm. Following this method, we fabricate uniform multiturn metallic nanohelices with heights and total lengths up to ∼1 μm in some cases.[14] To appreciate the structural relevance of regular and long metal nanohelices, we point out that the availability of nanohelices with multiple turns is a decisive factor to explore the wavelength scaling of the helical antenna at optical frequencies, which is the main purpose of our present work. In this context, we demonstrate that the operation of the metal nanohelices as plasmonic (optical) antenna is mainly determined by the existence of a longitudinal plasmon resonance (LSPR). In particular, we find the LSPR to follow a linear scaling-rule dependent on the total of all individual dipole effective-lengths appearing along the nanostructure at the plasmon resonance. That is, accounting for the total length of the nanohelix including pitch p, diameter D, and number of turns N. As stated above, this is in clear contrast with macroscopic helical helices, where the scaling of the axial resonant mode is only determined by the effective length of a

Received: February 19, 2015
Published: May 11, 2015

DOI: 10.1021/acsphotonics.5b00076
ACS Photonics 2015, 2, 675−679

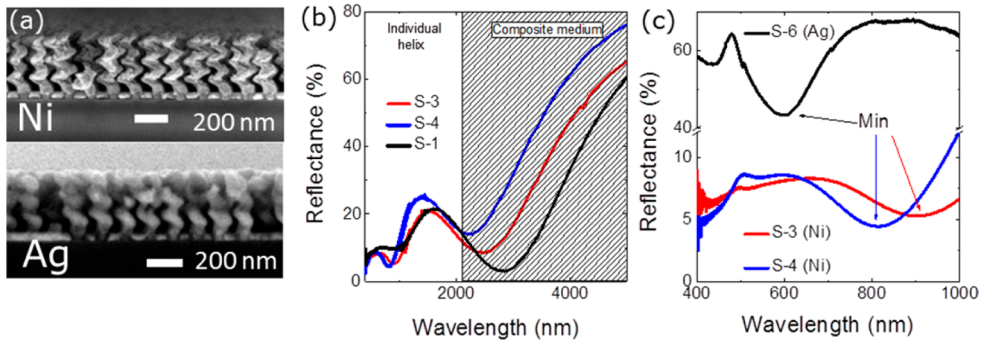

Figure 1. Morphology and reflectance of Ni and Ag nanohelices. (a) Scanning electron micrograph showing the side view of Ni (upper image, pitch p = 90 nm, diameter D = 90 nm) Ag nanohelices (lower image, p = 90 nm, D = 80 nm) and with multiple turns N. The wire radius of both samples is ~70 nm and is mainly determined by the seed spacing[14] (150 nm in our case). (b) Reflectance data from 400 to 5000 nm at normal incidence for arrays of nanohelices S-1, S-2, and S-3. Depending on the wavelength range, the reflectance is either dominated by an individual-particle or a composite-medium response (see Supporting Information). The transition to the effective-medium response is in all our samples approximately located at a wavelength > 2000 nm. (c) Experimental reflectance data from 400 to 1000 nm at normal incidence for samples S-3 (Ni, p = 128 nm, D = 72 nm, N = 3), S-4 (Ni, p = 63 nm, D = 59 nm, N = 3.7), and S-6 (Ag, p = 130 nm, D = 75 nm, N = 2.3). A complete description of the structural parameters of the samples used in this study is given in Table T1.[20] A well-developed minimum (Min) is observed from 600 to 900 nm.

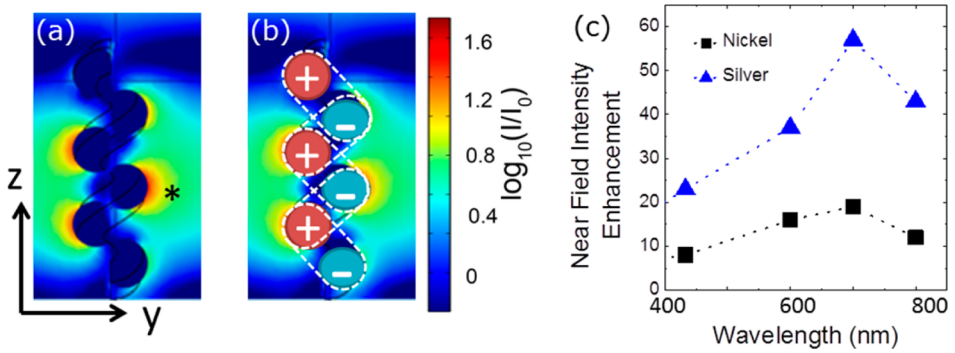

Figure 2. FEM simulations for Ni and Ag helices. (a) Near-field intensity in the x = 0 plane calculated using the FEM method for a Ni helix at incident monochromatic light (700 nm). (b) Representation of the dipole distribution along the helical structure with effective length $l/2$. (c) Intensity enhancement vs wavelength for nanohelices made from Ni and Ag at an arbitrary chosen point marked with (*) in (a). Ni shows the lowest intensity enhancement, which is attributed to the stronger plasmon-damping in ferromagnetic materials than in noble metals due to interband transitions.[16−19] In all the cases, the helix dimension used was p = 125 nm, D = 75 nm, N = 2.5. Dotted lines are a guide to the eye.

single dipole.[1] We also tested the material dependence of the LSPR by producing nanohelices from silver and nickel, two plasmonic materials[16,17] with very dissimilar interband activity in the optical spectrum.[18,19] In the case of silver nanohelices, we show that the decay of their longitudinal plasmon is radiative and the radiation preferably directed along the helical axis. In contrast, the plasmon decay in nickel nanostructures is dominated by a nonradiative damping. The latter observations demonstrate how the material choice allows an extra degree of freedom to control optical fields at the nanoscale with metallic helical nanostructures.

Structurally well-defined and freestanding nanohelices with multiple turns are shown in Figure 1a (growth details in ref 14 and Supporting Information). They possess uniform pitch and diameter (both varying below 10%, Table T1, Supporting Information), a key factor for optical antenna applications.[5] To characterize the basic optical properties of the metallic nanohelices, we first confirmed that they are optically active in the visible and near-infrared (NIR) spectra (details in ref 14 and Supporting Information), as expected for chiral particles.[20] In addition, we verify that the response from our nanohelical arrays is primarily due to the individual nanohelices at optical frequencies. Typically, for a given array of periodicity δ (150 nm in our case), the individual particle response prevails for wavelengths shorter than 10δ,[21] that is, below 1500 nm in the present case. We confirmed this fact in our samples by comparing specular-reflectance measurements in the wavelength range from 400 to 5000 nm for several samples and as a function of incident angle with their corresponding calculated reflectance (see Supporting Information). We point out that the employed analytical expression to calculate the reflectance comprises two contributions: scattering from single helices and effective-medium formalisms. In all the studied samples, the composite medium contribution is relevant at wavelengths >2000 nm (Figure 1b and ref 20), in agreement with the previously cited work[21] and ensuring that we can exclude spurious effects from the effective medium contribution in our wavelength region of interest.

Figure 1c shows the reflectance spectra for three typical samples made from silver and nickel within the individual particle range regime (400 to 1000 nm wavelength). Each spectrum is entirely due to the individual nanohelices response and not to a substrate effect (no transmission is possible in the measured wavelength range as the nanohelices are standing on a highly reflective several tens of nm thick Ag film).

Interestingly, despite the different absolute values of reflectance for the Ni and Ag nanohelices (Figure 1c), in all samples, the associated spectrum shows a minimum (Min) that

DOI: 10.1021/acsphotonics.5b00076
ACS Photonics 2015, 2, 675−679

is located at a wavelength coinciding with the total length, lN, of the wire forming an individual nanohelix (l is the length of one turn). This apparent structural dependence suggests the presence of a LSPR in the nanohelix at this associated wavelength. We complemented and confirmed these reflectance measurements conducting additional extinction measurements[22] in metallic nanohelices grown on a transparent ITO substrate (Supporting Information).

To gain a deeper understanding of the appearance of the reflectance minimum (maximum in extinction), we simulated the near-field intensity of Ni and Ag nanohelices (Figure 2a–c) and their far-field reflectance using the finite-element method (Supporting Information). When light is incident in the negative z-direction and linearly polarized in the y-direction (Figure 2a,b), we observe that the surface charge is accumulated along the nanohelix at positions separated by $l/2 = ((\pi D)^2 + p^2)^{1/2}/2$. This charge distribution is associated with the periodic formation of dipoles each of which with an effective length of $l/2$. Around the Min position, the near-field intensity is maximal in both Ni and Ag nanohelices (Figure 2c), proving that this reflectance minimum is associated with the formation of a plasmon resonance along the entire nanohelix, and thus, a LSPR with a resonant wavelength $\sim lN$. We note that a recent theoretical study on plasmonic nanohelices[23] suggests that the wavelength of this LSPR modes should scale linearly only with the effective length $l/2$ of one individual dipole. However, applying this theory[23] to our experimental results does not reveal a linear scaling with $l/2$ (inset Figure 3). Therefore, there must be a different plasmon-scaling in metal nanohelices which we attribute to multiple dipole coupling in the metallic nanostructures. Consequently, following our experimental observations, the LSPR wavelength in a nanohelix should scale as

$$\lambda_p \sim lN \tag{1}$$

To confirm this linear scaling, we plot (Figure 3) the experimental Min positions against lN for our 16 fabricated Ni and Ag nanohelix arrays and an additional ten numerically simulated nanohelix arrays both sets being in the same structural parameter range (Table T1, Supporting Information). The data points in the graph all lie on a straight line for each grown material, proving that the longitudinal plasmon wavelength scaling of metallic nanohelices is indeed described by eq 1 (additional confirmation is provided in the discussion of Figure 4a, below).

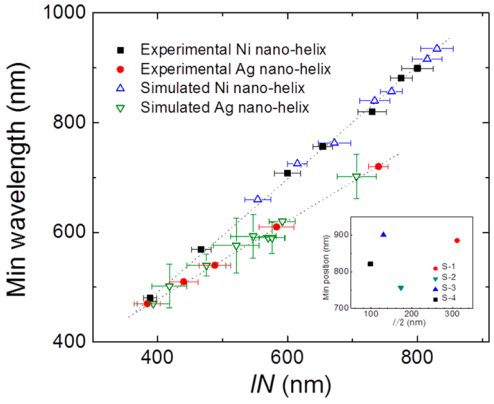

Figure 3. Scaling of the operation wavelength of the helical plasmonic antenna. Dependence of Min position on lN for experimentally measured and numerically simulated Ni and Ag nanohelices (Table T1, Supporting Information). A linear dependence is observed for all structures, proving that the longitudinal localized surface-plasmon of a nanohelix scales with lN, that is, following $\lambda_p \sim lN$ (eq 1). Data from simulated Ag nanohelices are taken from refs 23–26, showing a very good agreement with our experimental results. Dotted lines are a guide to the eye. We note that Ni and Ag nanohelices have a different slope in the scaling law that might be attributed to different plasmon decays in Ni and Ag at optical frequencies.[16−19] Inset: experimental data of samples S-1 to S-4 plotted according to the scaling-law proposed in ref 24 (effective length of one dipole), showing no match with our experimental data.

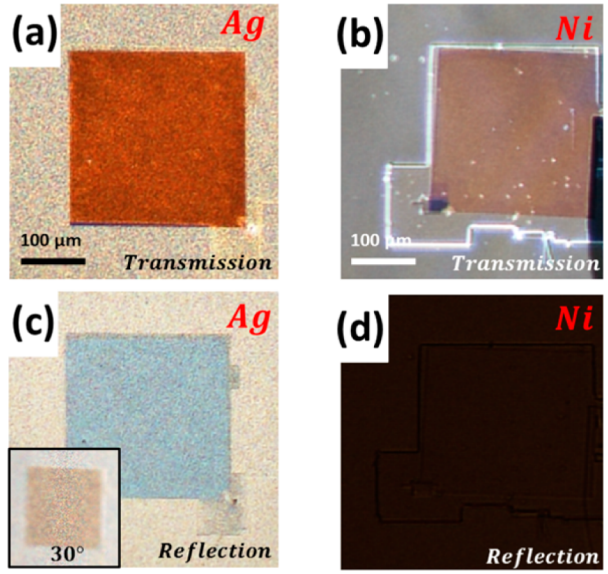

Figure 4. Longitudinal LSPR decay in Ag and Ni nanohelices. (a) Transmitted light through an array Ag nanohelices on ITO with an LSPR position in the blue ~470 nm (sample S-10 in Table T1, Supporting Information). The red color indicates either absorption or back scattering of blue light in the nanostructures. (b) Transmitted light through Ni nanohelices with a plasmon position of ~480 nm (sample S-11 in Table T1, Supporting Information). The red color indicates again a possible absorption or reflection of blue light (LSPR position). (c) Reflected light from Ag sample in (a) is in the blue showing a radiative plasmon damping. The inset shows that reflection at 30° is reddish, indicative of a directional decay of the blue LSPR parallel to the helical axis. (d) Reflected light from sample in (b). The black color in this case indicates a nonradiative decay of the LSPR in Ni resulting in light absorption. We note that outside the rectangle with regular nanohelices there are helical films deposited on the low thermal conductance layer (PMMA), which makes them irregular.[14] The color of these structures changes neither in reflection nor in transmission, demonstrating the importance of having regular nanohelices to observe the damping mechanism for different metals.

Furthermore, Figure 3 shows that this linear scaling law conciliates previously reported theoretical and numerical results on the plasmon scaling of metallic nanohelices in refs 23–26, where the presence of multiple turns N in the LSPR scaling was not considered in detail (mainly p and D were varied). Therefore, this longitudinal plasmon mode is determined by both the effective dipole length ($l/2$) and the number of dipoles in the structure ($\sim 2N$), whose product equals the total length of the wire defining the nanohelix. Our results are consistent within the wide parameter variations evaluated experimentally and numerically in the present study (N in the range of 1.1 to

DOI: 10.1021/acsphotonics.5b00076
ACS Photonics 2015, 2, 675−679

3.7, D and p varying from twice to eight times the wire radius). Within this parameter space, both main cases $D > p$ and $p > D$ were considered, together with the response from a noninteger N present in the nanostructures and different simulated wire thicknesses, that is, wire radii 10, 25, and 37 nm (see Supporting Information). We emphasize that this plasmon mode differs from the axial operation-mode in a conventional micro- and macrosized helical antenna.[1] In these conventional helical antennae, the mode resonance is close to $\sim l$,[1] thus, scales with the effective length of one dipole only.[1,23] In contrast, in our nanohelix case, the resonant wavelength of the longitudinal plasmon mode is N times larger due to the plasmon surface-charge-wave propagation along the entire helical structure. We note that, since the optical response of metallic nanohelices is governed by a localized plasmon, we expect the scaling to be valid in metals up to wavelengths ~ 1500 nm. The latter value corresponds to the maximum wavelength where the free electron density present in metals activates localized plasmons.[27]

Next, in the macroscopic case, antennas have resonances at wavelengths larger than the optical spectrum where all metals are mainly considered perfect conductors.[1] This is not the case in plasmonic nanoantennae, where the different types of metals play an important role in the optical properties of any nanostructure.[16,17] In particular, for a given shape and size, the presence of interband transitions in metals at optical frequencies are able to modify the plasmonic decay in the nanostructures.[16,28] Figure 4 shows transmission and reflectance optical microscope images of two similar nanohelix samples made from Ag and Ni with a total length of ~470 and ~480 nm, respectively, and defined on transparent ITO substrates. Equation 1 predicts that both samples have the longitudinal plasmon resonance situated in the blue of the visible spectrum (Figure 3). The transmission spectra of both types of nanohelices show a reddish color (Figure 4a,b), which is a consequence of the increased scattering and absorption at the plasmon wavelength (blue). The normal reflectance of regular Ag nanohelices (Figure 4c) shows a blue color, too. This demonstrates how the LSPR of the Ag nanohelices predominantly decays radiatively through scattering, in agreement with the absence of interband transitions in this metal at optical frequencies.[18] The inset of Figure 4c shows that at an angle of 30° away from the helical axis the Ag array shows a reddish color again, a fact that points toward a highly directional nature of the scattering along the helical axis. Meanwhile, the reflectance of regular Ni nanohelices is dark (Figure 4d). This is a consequence of a nonradiative damping[28] of the LSPR due to the interband activity present in this material at optical frequencies,[19] resulting in light absorption.[28]

In conclusion, the availability of multiple pitch and uniform metallic nanohelices allowed us to demonstrate the existence of a longitudinal LSPR in the nanohelix which determines its operation as optical helical antenna. The LSPR follows a linear scaling-rule dependent on the total effective length of all dipoles formed in the helical nanostructure at resonance. This is in contrast to micro- and macroscopic metallic helices where their resonance scales with the effective length of an individual dipole (single turn only). In addition, we demonstrated that in nickel nanohelices absorptive damping due to the interband activity is dominating, contrary to the case of silver nanohelices. This observation displays how the material choice allows an extra degree of freedom to control the optical fields at the nanoscale with plasmonic helical antennas. Finally, we showed that the radiative decay of the LSPR is strongly directional along the longitudinal axis of the nanohelix. These aspects enable the exploitation of helical nanostructures in a broad range of optical applications including photodetection, solar energy harvesting, and stealth technologies, as well as photothermal therapy and for sensors in biotechnology.

■ ASSOCIATED CONTENT

Supporting Information

Details about sample growth, reflectance and transmission measurements, finite element modeling, and optical activity. The Supporting Information is available free of charge on the ACS Publications website at DOI: 10.1021/acsphotonics.5b00076.

■ AUTHOR INFORMATION

Corresponding Author

*E-mail: vojislav.krstic@fau.de.

Notes

The authors declare no competing financial interest.

■ ACKNOWLEDGMENTS

This work was supported by the Science Foundation Ireland (TIDA 11/TIDA/I2031, CSET 08/CE/I1432, PI awards 08/IN.1/I1873, and 08/IN.1/I1862). We thank the Advanced Microscopy Laboratory, CRANN, TCD for assistance during sample preparation.

■ REFERENCES

(1) Balanis, C. A. Antenna Theory: Analysis and Design. Wiley & Sons: New York, 2005.
(2) Gansel, J. K.; Thiel, M.; Rill, M. S.; Decker, M.; Bade, K.; Saile, V.; von Freymann, G.; Linden, S.; Wegener, M. Gold helix photonic metamaterial as broadband circular polarizer. *Science* **2009**, *325*, 1513.
(3) Hagerty, J. A.; Helmbrecht, F. B.; McCalpin, W. H.; Zane, R.; Popovic, Z. B. Recycling ambient microwave energy with broad-band Rectenna Arrays. *IEEE Trans. Microwave Theory Tech.* **2004**, *52*, 1014.
(4) Novotny, L. Effective wavelength scaling for optical antennas. *Phys. Rev. Lett.* **2007**, *98*, 266802.
(5) Bjaradwaj, P.; Beutsch, B.; Novotny, L. Optical antennas. *Adv. Opt. Photonics* **2009**, *1*, 438.
(6) Bohren, C. F.; Huffman, D. R. *Light Scattering by Small Particles*; Wiley-Interscience: New York, 1983.
(7) Zorić, I.; Zäch, M.; Kesemo, B.; Langhammer, C. Gold, platinum and aluminium nanodisk plasmons: Material independence, subradiance and damping mechanisms. *ACS Nano* **2011**, *4*, 2535.
(8) Cao, W.; Huang, T.; Xu, X. H. Localized surface plasmon resonance of single silver nanoparticles studied by dark-field optical microscopy and spectroscopy. *J. Appl. Phys.* **2011**, *109*, 34310.
(9) Sekhon, J. S.; Verma, S. S. Rotational selection of nanorod plasmons: Material, size, and shape dependence mechanism for optical sensors. *Plasmonics* **2012**, *7*, 453−459.
(10) Hatab, N. A.; Hsueh, C.-H.; Gaddis, A. L.; Retterer, S. T.; Li, J.-H.; Eres, G.; Zhang, Z.; Gu, B. Freestanding optical gold Bowtie nanoantenna with variable gap size for enhanced Raman spectroscopy. *Nano Lett.* **2010**, *10*, 4952−4955.
(11) Taminiau, T. H.; Segerink, F. B.; Moerland, R. J.; Kuipers, L. K.; van Hulst, N. F. Near field driving of a monopole antenna. *J. Opt. A: Pure Appl. Opt.* **2007**, *9*, 315−321.
(12) Fischer, T.; Martin, O. J. F. Engineering the optical response of plasmonic nanoantennas. *Opt. Exp.* **2008**, *16*, 9144−9154.
(13) Kosako, T.; Kadoya, Y.; Hofmann, H. F. Directional control of light by a nano-optical Yagi−Uda antenna. *Nat. Photonics* **2010**, *4*, 312−315.

DOI: 10.1021/acsphotonics.5b00076
ACS Photonics 2015, 2, 675−679

(14) Caridad, J. M.; McCloskey, D.; Donegan, J. F.; Krstić, V. Controllable growth of metallic nano-helices at room temperature conditions. *Appl. Phys. Lett.* **2014**, *105*, 233114.
(15) Robbie, K.; Brett, M. J.; Lakhtaria, A. Chiral sculptured thin films. *Nature* **1996**, *384*, 616.
(16) Naik, G. V.; Shalaev, V. M.; Boltasseva, A. Alternative plasmonic materials: Beyond gold and silver. *Adv. Mater.* **2013**, *25*, 3264.
(17) Chen, J.; Albella, P.; Pirzadeh, Z.; Alonso-González, P.; Huth, F.; Bonetti, S.; Bonanni, V.; Åkerman, J.; Nogués, J.; Vavassori, P.; Dmitriev, A.; Aizpurua, J.; Hillenbrand, R. Plasmonic nickel nano-antennas. *Small* **2011**, *7*, 234.
(18) Ehrenreich, H.; Philip, H. R. Optical properties of Ag and Cu. *Phys. Rev.* **1962**, *128*, 1622.
(19) Ehrenreich, H.; Philip, H. R.; Olechna, D. J. Optical properties and fermi surface of nickel. *Phys. Rev.* **1963**, *131*, 2469.
(20) Barron, L. *Molecular Light Scattering and Optical Activity*; Cambridge: United Kingdom, 2004.
(21) Driscoll, T.; Smith, D. R.; Basov, D. N. Spectroscopic investigation of metamaterials across the effective medium threshold. *Metamaterials* **2010**, *4*, 175.
(22) Willets, K. A.; Van Duyne, R. P. Localized surface plasmon resonance spectroscopy and sensing. *Annu. Rev. Phys. Chem.* **2007**, *58*, 267.
(23) Zhang, Z. Y.; Zhao, Y. P. The visible extinction peaks of Ag nanohelixes: A periodic effective dipole model. *Appl. Phys. Lett.* **2011**, *98*, 083102.
(24) Larsen, G. K.; He, Y.; Wang, J.; Zhao, Y. Scalable fabrication of composite Ti/Ag plasmonic helices: Controlling morphology and optical activity by tailoring material properties. *Adv. Opt. Mater.* **2014**, 1.
(25) Zhang, Z. Y.; Zhao, Y. P. Optical properties of helical Ag nanostructures calculated by discrete dipole approximation method. *Appl. Phys. Lett.* **2007**, *90*, 221501.
(26) Zhang, Z. Y.; Zhao, Y. P. Optical properties of helical and multiring Ag nanostructures: The effect of pitch height. *J. Appl. Phys. Lett.* **2008**, *104*, 013517.
(27) Luther, J. M.; Jain, P. K.; Ewers, T.; Alivisatos, A. P. Localized surface plasmon resonances arising from free carriers in doped quantum dots. *Nat. Mater.* **2011**, *10*, 361.
(28) Sönnichsen, C.; Franzl, T.; Wilk, T.; von Plessen, G.; Feldmann, J.; Wilson, O.; Mulvaney, P. Drastic reduction of plasmon damping in gold nanorods. *Phys. Rev. Lett.* **2002**, *88*, 077402.

DOI: 10.1021/acsphotonics.5b00076
ACS Photonics 2015, 2, 675−679